Nanoscale

View Online
Dynamic Article Links

Cite this: *Nanoscale*, 2011, **3**, 2280

www.rsc.org/nanoscale

PAPER

Exciton diffusion and charge transfer dynamics in nano phase-separated P3HT/PCBM blend films†

Hai Wang,[ab] Hai-Yu Wang,*[a] Bing-Rong Gao,[a] Lei Wang,[ab] Zhi-Yong Yang,[ab] Xiao-Bo Du,[ab] Qi-Dai Chen,[a] Jun-Feng Song[a] and Hong-Bo Sun*[ab]

Received 18th December 2010, Accepted 6th March 2011
DOI: 10.1039/c0nr01002b

Exciton quenching dynamics has been systematically studied in pristine P3HT and nano phase separated P3HT/PCBM blend films under various excitation intensities by femtosecond fluorescence up-conversion technique. The behaviors of excitons in the films can be well described by a three-dimensional diffusion model. The small diffusion length and large charge transfer radius indicate that excitons reach the interface most likely by the delocalization of the excitons in P3HT fibrillar at a range of 4.8–9 nm so that the excitons can quickly delocalize in the P3HT domain to reach the interface (instead of by diffusion).

1. Introduction

Polymer solar cells have gained much academic and commercial attention for their advantages such as low cost, easy processing, light weight and flexibility. Recent achievement of power conversion efficiency over 7% from blends of low band gap polymers[1,2] solidifies their promising roles in industrial photovoltaic applications. For this purpose, a problem that needs to be addressed immediately is, why has such a high efficiency been achieved and how can it be further improved to the commercial threshold of 10%?[3] Answer to the question needs deep insight into photoconversion physics, on which, however, a lot of controversial experimental reports exist, particularly on the mechanisms of exciton diffusion and charge separation. Taking the electron donor/acceptor model system of regioregular poly(3-hexyl thiophene) (rr-P3HT) and phenyl-C61-buryric acid methyl ester (PCBM) as an example,[4–9] it has been found that thermal annealing of the P3HT/PCBM blend films leads to an increase of the power conversion efficiency. Morphological studies reveal phase separation of P3HT and PCBM in the annealed films (Scheme 1) with the fibrillar networks of P3HT crystals having a typical width of D_{Fib} = 13–15 nm,[10] and exhibiting repetitive elements within each unit consisting of an adjacent P3HT and PCBM.[11] The formation of nano scaled phase separation of about 13–15 nm in this system is found to be the most favorable morphology to produce high power conversion efficiency. The underlying physics is considered as a trade-off has been reached at this scale to ensure both charge transport and charge separation take place efficiently, since charge separation requires the close proximity of the donor and the acceptor, whereas charge transport requires phase separation to form a pathway for separated charges to reach the electrodes. It is commonly believed that in polymer solar cells excitons must diffuse to the interface to undergo charge separation. The diffusion model is now in doubt because the experimentally observed charge separation time is very short, typically at 8 ps,[12,13] which gives rise to a diffusion length of excitons of less than 2 nm, much less than that needed by most excitons to reach the interface for charge separation. Similar short diffusion length has been obtained by time-resolved microwave conductivity,[14]

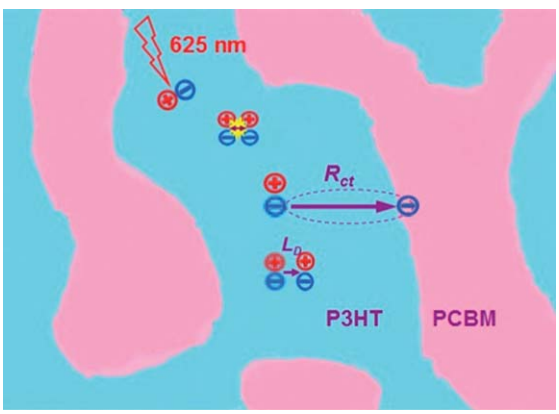

Scheme 1 Illustration of exciton generation, diffusion, annihilation and charge transfer dynamics in nano phase-separated P3HT/PCBM blend films. L_D is the diffusion length in a certain time, R_{CT} is the charge transfer radius.

[a]*State Key Laboratory on Integrated Optoelectronics, College of Electronic Science and Engineering, Jilin University, 2699 Qianjin Street, Changchun, 130012, China. E-mail: haiyu_wang@jlu.edu.cn; hbsun@jlu.edu.cn*
[b]*College of Physics, Jilin University, 119 Jiefang Road, Changchun, 130023, China*

† Electronic supplementary information (ESI) available: Calculation of the excitation density, solution of fitting equation. See DOI: 10.1039/c0nr01002b

pump–probe,[15] and time-resolved fluorescence technique[16] studies. In order to interpret the contradiction between the experimentally observed large size (13–15 nm) of the P3HT nanophase and short diffusion length (~2 nm in 8 ps) of excitons to realize efficient charge separation, alternative mechanisms have been proposed, for example, delocalization of excitons into a large area to efficiently reach the whole P3HT domain,[12,13] or energy transfer from the P3HT singlet excited state to PCBM, although quantitative experimental support is still lacking. Synthesis of better photovaltic polymer materials or design of novel device structures of solar cells with higher power conversion efficiency would be less efficient without a thorough understanding of the dynamics of exciton diffusion and charge separation.

Time resolved spectroscopy is a powerful tool to investigate the key photophysical processes in materials,[17–22] and it has been extensively applied to study the P3HT/PCBM system.[13,23–27] In this paper, we report a systematic study of exciton quenching dynamics in pristine P3HT and P3HT/PCBM blends under varied excitation intensities by femtosecond fluorescence up-conversion technique. The technology provides a clean probe of the exciton dynamics without interfering with the signals from the excited state absorption or ground state bleaching. The quenching of photogenerated excitons is therefore due to either exciton-exciton annihilation or charge transfer to the acceptor. This makes it possible to quantitatively determine the charge transfer radius R_{CT} in the bulk heterojunction for the first time. A comparison of R_{CT} and the diffusion length provides quantitative information on the significance of the role played by exciton diffusion on charge separation.

2. Experiments

PCBM and Regioregular P3HT with Mw = 60k and regioregularity greater than 95% were purchased from Luminescence Technology Corp. and used without further purification. Dichlorobenzene solution of P3HT with a concentration of 30 mg mL^{-1} was heated to a temperature of approximately 50 °C until all samples were dissolved. The solution was then ultrasonic oscillated for 4 min. The solution was spin-coated onto a quartz substrate, annealed at 150 °C for 30 min and was sealed between two quartz slides. The peak absorbance of the films is about 0.5. To avoid degradation by oxygen, the spin-coating and sealing processes were done under nitrogen environment in a glove box with an oxygen concentration smaller than 0.1 ppm. For the P3HT/PCBM blend films, P3HT and PCBM of different weight ratios (50 wt%, 23 wt%, 2.5 wt% PCBM) were put into dichlorobenzene with a concentration of 20 mg mL^{-1}, and then stirred at a temperature of approximately 50 °C for 2 h. The same processes were used for preparing the P3HT films.

Absorption spectra were measured using a Shimadzu UV-1700 spectrophotometer with a 1 nm resolution. Emission spectra were recorded with an AvaSpec-2048 fiber optic spectrometer at a 0.6 nm resolution.

Nanosecond fluorescence lifetime experiments were performed by a time-correlated single photon counting (TCSPC) system under a right-angle sample geometry. A 379 nm picosecond diode laser (Edinburgh Instruments EPL375, repetition rate 20 MHz) was used to excite the samples. The fluorescence was collected by a photomultiplier tube (Hamamatsu H5783p) connected to a TCSPC board (Becker&Hickel SPC-130). Time constant of the instrument response function (IRF) is about 220 ps.

Sub-picosecond time resolved emission was measured by the femtosecond fluorescence up-conversion method. The setup has been described in detail elsewhere.[28] In brief, a Nd:YVO_4 laser (Millennia, Spectra Physics) was used to pump a Ti:Sapphire laser (Tsunami, Spectra Physics). Its output seeds a regenerative amplifier (RGA, Spitfire, Spectra Physics). The output of the amplifier of 1.5 mJ pulse energy, 100 fs pulse width, at 800 nm was split into two parts. One was used to pump an optical parametric amplifier (OPA) to generate excitation pulses at 625 nm. The resulting fluorescence was collected and focused onto a 1 mm thick BBO crystal with a cutting angle of 35 degrees. The other part of the RGA output was sent into an optical delay line and served as the optical gate for the up-conversion of the fluorescence. The generated sum frequency light was then collimated and focused into the entrance slit of a 300 mm monochromator. A UV-sensitive photomultiplier tube 1P28 (Hamamatsu) was used to detect the signal. The electrical signal from the photomultiplier tube was summed by a digital oscilloscope. The relative polarization of the excitation and the gating beams was set at the magic angle. The FWHM of instrument response function was about 450 fs. All the measurements were preformed at room temperature.

3. Results and discussion

3.1 Steady state spectra

P3HT pristine film and P3HT/PCBM blend films with three different PCBM loadings were prepared. The steady state absorption and fluorescence emission spectra are shown in Fig. 1 (a) and (b). The absorption shoulder around 600 nm (0-0 vibronic) is a characteristic feature indicative of formation of the crystalline form of P3HT as a result of annealing. The fluorescence is efficiently quenched by the addition of PCBM, *e.g.* more than 95% of the fluorescence was quenched in the blend film with 50 wt% PCBM.

3.2 Exciton dynamics and the fitting model

All time-resolved experiments have been conducted under red edge excitation at 625 nm to minimize the effect of intrachain and interchain energy transfer.[17,29] We are only interested in the quenching process under various excitation intensities, but energy transfer from higher energy segment to lower energy segment will result in a spectral red shift: faster decay for the blue side of the photoluminescence (PL) spectra and a rise component for the red side, making the photoluminescence dynamics more complicated to analyze. Instead, red edge excitation already excites the low energy segments of P3HT, and thus can minimize the interfering effect of downhill energy transfer. We choose the emission peak of 710 nm as the probe wavelength to further minimize this effect, for the peak dynamics is least affected by the energy transfer. The red edge excitation can also avoid prompt charge separation, as the 625 nm excitation can only generate singlet excitons in the core crystalline region but cannot excite the relatively disordered interface region.[13] For each film,

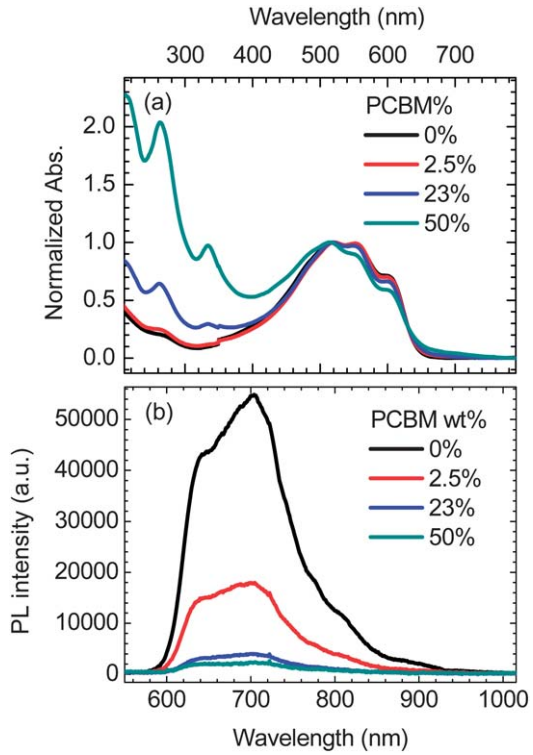

Fig. 1 Steady state (a) absorption spectra normalized at 520 nm, and (b) fluorescence emission spectra (the excitation wavelength was 405 nm) of rr-P3HT and P3HT/PCBM blend films.

fluorescence dynamics under five different excitation intensities were measured. For pristine P3HT, the fluorescence kinetics shows a strong power dependence which is mainly due to the exciton-exciton annihilation (Fig. 2). At high excitation densities when excitons are able to interact with each other, a pair of annihilation excitons fuses to form a higher energy exciton. The dominant relaxation pathway of the high energy exciton is found to be the internal conversion to the lowest excited state,[30] so one excition is lost per interaction. The loss of excitons to annihilation is dependent on the excitation density and results in a faster

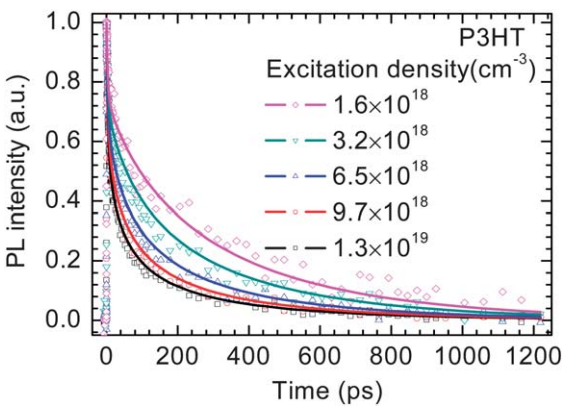

Fig. 2 The experimental data (open symbols) and fits (solid lines) for the fluorescence dynamics of the P3HT film under various excitation densities. Initial exciton density is given. The excitation wavelength is 625 nm and the probe wavelength is 710 nm.

decay of the fluorescence at higher excitation density. In the blend films, the fluorescence is further quenched by charge transfer processes. For the 50 wt% PCBM sample (Fig. 3(c)), the kinetics exhibit much less excitation intensity dependence than that of the pristine P3HT, indicating that the charge transfer becomes the dominating process in the blend films. Most of the excitons dissociate to charges before they annihilate, resulting in little influence of the excitation intensity. The longest lifetime is about 40 ps, which is consistent with the values in other reports.[31,32]

To get a quantitative analysis of the exciton dynamics, we assume that the two main quenching channels are exciton-exciton annihilation and charge transfer process in the blend films. The rate equation is written as:

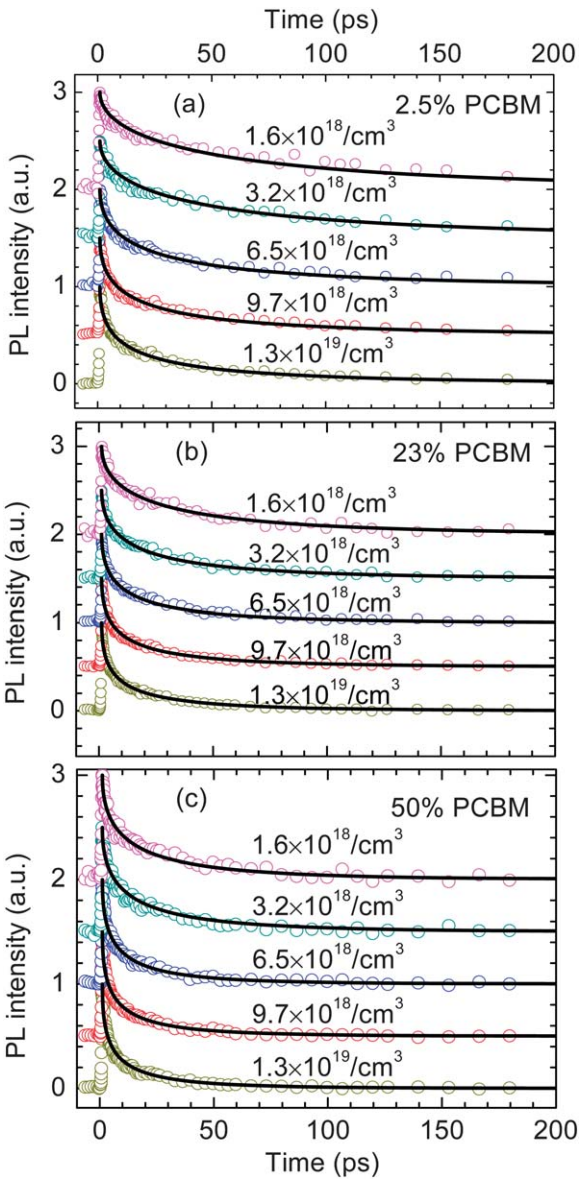

Fig. 3 The experimental data (open circles) and fits (solid lines) for the fluorescence dynamics of the (a) 2.5 wt% (b) 23 wt% and (c) 50 wt% PCBM blend films under various excitation densities. Initial exciton density is given. The excitation wavelength is 625 nm and the probe wavelength is 710 nm.

$$\frac{dN(t)}{dt} = -\frac{N(t)}{\tau_0} - k_{EEA}(t)N(t)^2 - k_{CT}(t)N_{CT}N(t) \quad (1)$$

where $N(t)$ is the exciton density; N_{CT} is the density of the acceptor PCBM; τ_0 is the intrinsic exciton lifetime, which was determined to be 450 ps by the time-correlated single photon counting experiment; k_{EEA} and k_{CT} are the exciton-exciton annihilation and the charge transfer rate constants, respectively. We adopt three-dimensional diffusion model, in which excitons have an isotropic diffusion constant D, and annihilation happens when a pair of excitons comes closer than a critical distance R_a. The critical distance for a charge transfer state is denoted R_{CT}. The time dependent rate constants are given as:[33–35] $k_{EEA} = 4\pi R_a D\left(1 + R_a/\sqrt{2\pi Dt}\right)$ and $k_{CT} = 4\pi R_{CT} D(1 + R_{CT}/\sqrt{\pi Dt})$.

The equation can be analytically solved by substituting in $M(t) = N(t)^{-1}$ and following the standard procedure for the emerging linear differential equation with an inhomogeneity. (See Supporting Information for details†) The solution is shown in eqn (2), where $\gamma_1 = 4\pi R_{CT} D N_{CT}$, $\gamma_2 = 4\pi R_a D N_0$, $\beta_1 = 4\sqrt{\pi D R_{CT}^2}\, N_{CT}$, $\beta_2 = 4\sqrt{\pi D/2 R_a^2}\, N_0$. The solution is used for the fitting of the fluorescence kinetics.

3.3 Exciton dynamics of the pristine P3HT film

For pristine P3HT film (Fig. 2), the photoinduced excitons will undergo annihilation at high excitation densities when excitons are close enough to interact with each other. Since there is no loading of PCBM ($N_{CT} = 0$), so there is no charge transfer, $\gamma_1 = 0$, $\beta_1 = 0$. The fluorescence quenching is only caused by excition-exciton annihilation. N_0 can be decided by calculating the exciton densities under varied excitation intensites. The fitting parameters are R_a and D. A globe fitting of all five kinetic curves gives the best fitting parameters of $R_a = 2.5 \pm 0.3$ nm and $D = (2.7 \pm 0.4) \times 10^{-4}$ cm^2 s^{-1}. Taking the exciton lifetime τ of 450 ps, the diffusion length is then estimated to be $L_D = \sqrt{D\tau_0} = 3.5 \pm 0.3$nm, which is in the range of 2.6–8.5 nm obtained by different experiments.[14–16] Our annihilation rate constant $\gamma = 4\pi R_a D = 8.5 \times 10^{-10}$ cm^3 s^{-1} is smaller than the value of 4.0×10^{-9} cm^3 s^{-1}, as reported by a similar fluorescence measurement.[16] We noticed that during their fitting, a long time approximation was taken, in which only data after 100 ps were used. We therefore tried the same long time approximation, the best fitting value of γ was found to be 2.5×10^{-9} cm^3 s^{-1}, closer but still smaller than their value. So we speculate that the long time approximation may cause an overestimation of the annihilation rate and diffusion length. From our value of diffusion coefficient, the excitons can only diffuse about 0.5 nm in 8 ps, which indicates that the exciton diffusion to the interface is too slow to give an efficient charge separation.

3.4 Exciton dynamics of the P3HT/PCBM blend films

Now we consider the blend samples in which the quenching of the fluorescence is not only caused by the bimolecular exciton annihilation, but also the charge transfer from P3HT to PCBM. To fit the fluorescence dynamics in the blend films, R_a and D were fixed to the values obtained from the fitting of the pristine P3HT film. In order to obtain a value of R_{CT}, we must know the PCBM density N_{CT}. However, the annealing of the blend films causes the phase separation of P3HT and PCBM, and the PCBM molecule does not homogeneously disperse in the film. Therefore, the density of PCBM can't be simply calculated by using the molecule number divided by the volume of the film. Thus we used the previously reported domain sizes of P3HT and PCBM to estimate the maximum distance between a P3HT and a PCBM molecule to calculate the effective PCBM density N_{CT}. Recent morphological studies of the blend films have revealed that the fibrillar networks of P3HT crystals have typical widths of 13–15 nm.[10] Since the film morphology changes with processing conditions, the domain size may vary for different experimental conditions, but a width of around 10 nm is commonly accepted.[12] For an upper limit of 15 nm, the maximum distance for a P3HT exciton to find the nearest PCBM molecule is 7.5 nm, which is measured from the center of the P3HT fibrillar to the heterojunction interface. Then the probability for a P3HT exciton finding a PCBM molecule is the same as a PCBM molecule dispersion with half the cube diagonal of 7.5 nm. Under this consideration, the calculated effective density will be 1.57×10^{18} cm^{-3}. Now the only free parameter is R_{CT}. For the blend films with 50 wt% PCBM, all the fluorescence kinetics for five excitation intensities can be well fitted with $R_{CT} = 9.0 \pm 0.6$ nm (Fig. 3(c)). If we consider the lower limit of the width of P3HT fibrillar to be 10 nm, corresponding to an effective PCBM density of 5.2×10^{18} cm^{-3}, then a value $R_{CT} = 4.8 \pm 0.4$ nm was obtained from fitting all kinetics simultaneously. For the intermediate P3HT domain width of 13 nm, values $R_{CT} = 7 \pm 0.6$ nm were obtained. Having got the R_{CT} in the 50 wt% blend film, we further examine whether the same R_{CT} value applies for the blend films of 23 wt% and 2.5 wt% PCBM. In the latter two blend films, less PCBM was added, so the P3HT size after annealing should be larger compared to the 50 wt% blend film, and the effective N_{CT} should be smaller. It is obvious that the exciton dynamics are slower (Fig. 3). We use the intermediate value of $R_{CT} = 7$ nm from the 50 wt% blend film to fit the data for the two blend films, leaving N_{CT} as the only free parameter. Satisfactory fits for all kinetics were obtained (Fig. 3(a), (b)), which proves that the same R_{CT} could apply for all the blend films with different PCBM loading. The fittings gave the effective PCBM densities of 1.18×10^{18} cm^{-3} for 23 wt% and 0.7×10^{18} cm^{-3} for 2.5 wt% PCBM loading, respectively. It is worth noting that owing to the phase separation, the effective PCBM density is no longer linearly dependent on the PCBM loading; instead, it all depends on the scale of the phase separation.

So far, we have obtained the R_{CT} values ranging from 4.8 nm to 9 nm according to different reported domain sizes. Because the exact value of N_{CT} is very difficult to know, R_{CT} obtained by the fitting is only estimation. However, the fitting results suggest that R_{CT} could be quite large, compared to the exciton diffusion length of less than 0.5 nm in P3HT for the first 8 ps. R_{CT} is the largest distance between the exciton and the acceptor for which charge transfer could occur. This means that even if an exciton generated in P3HT is up to 9 nm away from the P3HT/PCBM interface, charge transfer could possibly take place (Scheme 1). Note that the range of R_{CT} (4.8–9 nm) almost covers half of the domain size of P3HT (5–7.5 nm), which means that most of the excitons can undergo efficient charge transfer, which is consistent with the observed high external quantum efficiency of over 80%.

$$N(t) = N_0 \exp\left(-\frac{t}{\tau_0} - \gamma_1 t - 2\beta_1\sqrt{t}\right)\left\{1 + \frac{\gamma_2}{\frac{1}{\tau_0}+\gamma_1}\left[1 - \exp\left(-\frac{t}{\tau_0} - \gamma_1 t - 2\beta_1\sqrt{t}\right)\right] + \sqrt{\frac{\pi}{\frac{1}{\tau_0}+\gamma_1}}\left(\beta_2 - \frac{\beta_1\gamma_2}{\frac{1}{\tau_0}+\gamma_1}\right)\exp\left(\frac{\beta_1^2}{\frac{1}{\tau_0}+\gamma_1}\right)\left[erf\left(\sqrt{\frac{t}{\tau_0}+\gamma_1 t} + \frac{\beta_1}{\sqrt{\frac{1}{\tau_0}+\gamma_1}}\right) - erf\left(\frac{\beta_1}{\sqrt{\frac{1}{\tau_0}+\gamma_1}}\right)\right]\right\} \quad (2)$$

Comparison of the small diffusion length and the large R_{CT} value confirms that the high charge separation efficiency could not be achieved by diffusion alone. The large R_{CT} could be possibly due to either energy transfer between P3HT and PCBM, or the delocalization of P3HT exciton at a range of R_{CT} (4.8–9 nm) in P3HT fibrillar. Samuel's group[36] has suggested that energy transfer from P3HT to PCBM promotes excitons to the interface, where they dissociate to charge carriers. However other work[23] suggested that energy transfer from ^{1}P* to ^{1}PCBM* is likely to be less efficient for thiophene polymer class compared to more emissive polymers such as polyfluorenes. If energy transfer could contribute in the charge separation, it would raise the question whether it can achieve such a high efficiency given the low emission of P3HT film and the small spectral overlap between the P3HT fluorescence emission and PCBM absorption. Alternatively Friend's group[12] suggested that excitons are delocalized and, hence, may sample ordered domains efficiently in tens of picoseconds. While another work[37] suggests that the delocalization radius of singlet exciton is 6.7 nm in the core RR-P3HT crystal, which is consistent with our value of R_{CT}. Therefore, we may reach a conclusion that exciton delocalization over a large area is a more possible explanation for the large R_{CT}. In this work, we didn't do excitation wavelength dependent estimation of the diffusion length and the charge transfer radius because we believe that the red edge excitation of 625 nm is representative enough. Higher energy excitation will excite both the aggregated and unaggregated region,[27] while the excitation of the unaggregated region quickly transfers to excite the aggregated region within the system resolution. It is reasonable to assume that the following diffusion process is the same as exciting the aggregate region only. When PCBM is added, the excitation of the unaggregated P3HT molecules may result in prompt charge separation to the PCBM molecule in close proximity, however R_{CT} in this work is only related to the excitons that need to travel a certain distance to reach the donor/acceptor interface, so the prompt charge separation does not affect R_{CT}. Furthermore, McGehee's group[38] reported that without consideration of PCBM absorption, the internal quantum efficiencies (IQEs) should be independent of excitation wavelength, which indicate that the following exciton diffusion and charge separation process after photoexcitation are not obviously excitation wavelength dependent.

4. Conclusions

In summary, our femtosecond fluorescence up-conversion experiments performed in pristine P3HT and nano phase-separated P3HT/PCBM blend films have shown that the exciton behaviors can be well described by a three-dimensional diffusion model. The fitting results suggest for the first time a range of R_{CT} from 4.8 nm to 9 nm. The large R_{CT} value and the small diffusion length indicate that excitons reach the donor/acceptor interface most likely by the delocalization of the excitons in P3HT fibrillar at a range of 4.8–9 nm so that the excitons can quickly sample P3HT domain to reach the interface (instead of by diffusion). Although energy transfer is another possibility, it may not be that efficient. Further study is required to distinguish between the two proposed mechanisms. It is necessary to quantify the efficiency of energy transfer and provide further evidences of exciton delocalization in such a large area. The elucidation of the different roles that are played by each process is crucial to understanding the fundamental physics of charge separation in polymer solar cells.

Acknowledgements

The authors would like to acknowledge the financial support from National Science Foundation of China (Grants number 21003060, 20973081 and 61076054).

References

1 H. Y. Chen, J. H. Hou, S. Q. Zhang, Y. Y. Liang, G. W. Yang, Y. Yang, L. P. Yu, Y. Wu and G. Li, *Nat. Photonics*, 2009, **3**, 649–653.
2 Y. Y. Liang, Z. Xu, J. B. Xia, S. T. Tsai, Y. Wu, G. Li, C. Ray and L. P. Yu, *Adv. Mater.*, 2010, **22**, E135–138.
3 B. R. Saunders and M. L. Turner, *Adv. Colloid Interface Sci.*, 2008, **138**, 1–23.
4 H. Hoppe and N. S. Sariciftci, *J. Mater. Chem.*, 2006, **16**, 45–61.
5 W. L. Ma, P. K. Iyer, X. Gong, B. Liu, D. Moses, G. C. Bazan and A. J. Heeger, *Adv. Mater.*, 2005, **17**, 274–1622.
6 G. Li, V. Shrotriya, J. S. Huang, Y. Yao, T. Moriarty, K. Emery and Y. Yang, *Nat. Mater.*, 2005, **4**, 864–868.
7 Y. Kim, S. Cook, S. M. Tuladhar, S. A. Choulis, J. Nelson, J. R. Durrant, D. D. C. Bradley, M. Giles, I. Mcculloch, C. S. Ha and M. Ree, *Nat. Mater.*, 2006, **5**, 197–203.
8 L. M. Chen, Z. R. Hong, G. Li and Y. Yang, *Adv. Mater.*, 2009, **21**, 1434–1449.
9 S. Sista, Z. R. Hong, M. H. Park, Z. Xu and Y. Yang, *Adv. Mater.*, 2010, **22**, E77.
10 X. N. Yang, J. Loos, S. C. Veenstra, W. J. H. Verhees, M. M. Wienk, J. M. Kroon, M. A. J. Michels and R. A. J. Janssen, *Nano Lett.*, 2005, **5**, 579–583.
11 W. L. Ma, C. Y. Yang and A. J. Heeger, *Adv. Mater.*, 2007, **19**, 1387.
12 R. A. Marsh, J. M. Hodgkiss, S. Albert-Seifried and R. H. Friend, *Nano Lett.*, 2010, **10**, 923–930.
13 J. M. Guo, H. Ohkita, H. Benten and S. Ito, *J. Am. Chem. Soc.*, 2010, **132**, 6154–6164.
14 J. E. Kroeze, T. J. Savenije, M. J. W. Vermeulen and J. M. Warman, *J. Phys. Chem. B*, 2003, **107**, 7696–7705.
15 L. Luer, H. J. Egelhaaf, D. Oelkrug, G. Cerullo, G. Lanzani, B. H. Huisman and D. de Leeuw, *Org. Electron.*, 2004, **5**, 83–89.
16 P. E. Shaw, A. Ruseckas and I. D. W. Samuel, *Adv. Mater.*, 2008, **20**, 3516–3520.

17 T. Q. Nguyen, J. J. Wu, V. Doan, B. J. Schwartz and S. H. Tolbert, *Science*, 2000, **288**, 652–656.
18 H. Y. Wang, S. Lin, J. P. Allen, J. C. Williams, S. Blankert, C. Laser and N. W. Woodbury, *Science*, 2007, **316**, 747–750.
19 Y. Jiang, H. Y. Wang, L. P. Xie, I. R. Gao, L. Wang, X. L. Zhang, Q. D. Chen, H. Yang, H. W. Song and H. B. Sun, *J. Phys. Chem. C*, 2010, **114**, 2913–2917.
20 L. M. Fu, X. F. Wen, X. C. Ai, Y. Sun, Y. S. Wu, J. P. Zhang and Y. Wang, *Angew. Chem., Int. Ed.*, 2005, **44**, 747–750.
21 K. Kanemoto, Y. Imanaka, I. Akai, M. Sugisaki, H. Hashimoto and T. Karasawa, *J. Phys. Chem. B*, 2007, **111**, 12389–12394.
22 M. Glasbeek and H. Zhang, *Chem. Rev.*, 2004, **104**, 1929–1954.
23 H. Ohkita, S. Cook, Y. Astuti, W. Duffy, S. Tierney, W. Zhang, M. Heeney, I. McCulloch, J. Nelson, D. D. C. Bradley and J. R. Durrant, *J. Am. Chem. Soc.*, 2008, **130**, 3030–3042.
24 I. W. Hwang, D. Moses and A. J. Heeger, *J. Phys. Chem. C*, 2008, **112**, 4350–4354.
25 K. Kanemoto, M. Yasui, D. Kosumi, A. Ogata, M. Sugisaki, T. Karasawa, I. Akai and H. Hashimoto, *Phys. Rev. Lett.*, 2009, **103**.
26 E. Lioudakis, I. Alexandrou and A. Othonos, *Nanoscale Res. Lett.*, 2009, **4**, 1475–1480.
27 J. Clark, C. Silva, R. H. Friend and F. C. Spano, *Phys. Rev. Lett.*, 2007, **98**, 206406.
28 B. R. Gao, H. Y. Wang, Y. W. Hao, L. M. Fu, H. H. Fang, Y. Jiang, L. Wang, Q. D. Chen, H. Xia, L. Y. Pan, Y. G. Ma and H. B. Sun, *J. Phys. Chem. B*, 2010, **114**, 128–134.
29 N. P. Wells, B. W. Boudouris, M. A. Hillmyer and D. A. Blank, *J. Phys. Chem. C*, 2007, **111**, 15404–15414.
30 Y. Zaushitsyn, V. Gulbinas, D. Zigmantas, F. L. Zhang, O. Inganas, V. Sundstrom and A. Yartsev, *Phys. Rev. B: Condens. Matter Mater. Phys.*, 2004, **70**, 075202.
31 J. Piris, T. E. Dykstra, A. A. Bakulin, P. H. M. van Loosdrecht, W. Knulst, M. T. Trinh, J. M. Schins and L. D. A. Siebbeles, *J. Phys. Chem. C*, 2009, **113**, 14500–14506.
32 D. Jarzab, F. Cordella, M. Lenes, F. B. Kooistra, P. W. M. Blom, J. C. Hummelen and M. A. Loi, *J. Phys. Chem. B*, 2009, **113**, 16513–16517.
33 E. Engel, K. Leo and M. Hoffmann, *Chem. Phys.*, 2006, **325**, 170–177.
34 M. V. Smoluchowski, *Z. Physik. Chemie*, 1917, **92**, 129.
35 S. Schandrasekhar, *Rev. Mod. Phys.*, 1943, **15**, 1.
36 A. Ruseckas, P. E. Shaw and I. D. W. Samuel, *Dalton Trans.*, 2009, 10040–10043.
37 J. M. Guo, H. Ohkita, H. Benten and S. Ito, *J. Am. Chem. Soc.*, 2009, **131**, 16869–16880.
38 G. F. Burkhard, E. T. Hoke, S. R. Scully and M. D. McGehee, *Nano Lett.*, 2009, **9**, 4037–4041.